

Petrophysical Analysis of the Green River Formation, Colorado—a Case Study in Oil Shale Formation Evaluation¹

Christopher Skelt²

ABSTRACT

The Green River formation in Southwestern Colorado is known as one of the world's richest oil shales and is the target for several oil companies' programs aimed at developing and evaluating technology to assess and develop the resource. Petrophysical evaluation of the potential liquid hydrocarbon yield is challenging due to the complex mineralogy that includes high and variable concentrations of minerals seldom encountered in conventional reservoirs. We present a case study of the evaluation of a comprehensive wireline and core data set that included natural, capture and inelastic gamma-ray spectroscopy, and NMR logs, and approximately twelve hundred feet of core-derived elemental and mineralogical analysis supplemented by Fischer Assays and RockEval pyrolysis measurements of the liquid hydrocarbon content.

The borehole was shallow, on gauge and filled with a low salinity drilling fluid, and the logs were acquired slowly, in conditions particularly suitable for good spectroscopy log quality. The dataset therefore offered an opportunity to assess the relative accuracy of the elemental yields from natural and induced gamma-ray spectroscopy in the most favorable conditions likely to be encountered

in oilfield operations, and as such represents a valuable reference for more general use of these logs. We showed that the match between wireline and core derived elemental concentrations varied considerably from element to element, and used this information to select the elements used as inputs in the detailed mineralogical analysis that followed.

This volumetric compositional analysis into minerals and organic matter was used as a starting point for reproducing Fischer Assay results, the recognized standard for quantifying liquid potential. This step included transformation from liquid hydrocarbon in gallons per ton of the assay samples to the more familiar barrels per acre-foot of the gross rock volume.

Finally, liquid hydrocarbon potential was estimated using simple overlays of square root conductivity against density and compressional slowness to compare the prediction accuracy achievable with a limited data set available in most regional wells against the standard obtained with the comprehensive data set used for the initial detailed evaluation.

INTRODUCTION

Spectroscopy logs were introduced (Grau et al., 1989) over twenty years ago, and many papers have been published showing results, accompanied by the sometimes dubious and rarely proven claim that sound log analysis would have been impossible without the aid of the spectroscopy data. Furthermore, although the primary output from the tools is the relative mass fractions of a collection of elements, these are rarely validated. This paper contains a rare independent (see also van den Oord, 1991) comparison of wireline spectroscopy-derived elements against core data, and comparison between estimation of oil shale liquid yield from a comprehensive logging suite and a standard suite of resistivity, density, neutron, sonic and gamma ray logs.

Core derived elemental yields were measured on two sets of samples—core plug offcuts, and trenched samples taken from approximately one foot intervals of the whole core—by inductively coupled plasma (ICP) atomic emission spectroscopy. Mineralogy was determined using Chevron's proprietary QXRD method of phase analysis by X-ray diffraction (Omotoso et al., 2006).

The spectroscopy data are from Schlumberger's Elemental Capture Sonde (ECS) that was part of a wireline suite that also included array induction, density, thermal neutron, natural gamma spectroscopy, nuclear magnetic resonance, sonic waveforms and micro-resistivity images. The logs were run in a well drilled by Chevron in Colorado in support of a research program aimed at commercially developing the Green River oil shale formation. The goal of this exercise

Manuscript received by the Editor June 20, 2011; revised manuscript received August 26, 2011.

¹Originally presented at the SPWLA 51st Annual Logging Symposium, Perth, Australia, June 19–23, 2010.

²Chevron Energy Technology Company, 1500 Louisiana Street, Houston, Texas, 77002, USA; Email: cskelt@chevron.com
©2011 Society of Petrophysics and Well Log Analysts. All Rights Reserved.

TABLE 1: Core data used in study.

	Method	Samples
Element Concentrations	ICP on plug off-cuts	69
Element Concentrations	ICP on whole core trenched samples	85
Mineralogy	QXRD	69
Mineralogy	QXRD on whole core trenched samples	85
Fischer Assay	ASTM D-3904	143
RockEval	Pyrolysis, flame ionization detector	ca 500

was to use all the relevant log and core data to build a petrophysical model to quantify inorganic mineralogy, organic matter and porosity from the wireline logs.

Borehole conditions were benign—fresh water in the on-gauge borehole and moderate formation temperature—and the logs were run slowly, resulting in spectra that are as high quality as can realistically be expected to be recorded. However, this does not necessarily imply that the accuracy of the computed elements is the best that may be encountered, because mineralogical diversity complicates the processing. Nonetheless this exercise should be a rigorous test of high quality raw data in complex mineralogy.

AVAILABLE DATA

The following wireline logs from Schlumberger were used in this study: array induction, litho density, thermal neutron, natural gamma spectroscopy, capture and inelastic spectroscopy and nuclear magnetic resonance.

Core data included mineralogy from X-ray diffraction, elemental chemistry, Fischer Assays and RockEval pyrolysis. The XRD and elemental data are from a combination of plugs and trenched samples. See Table 1. Core data analysis was concentrated in several zones of interest, and sparse over the rest of the studied interval.

The hole was on gauge throughout, and the combination of low salinity, low density drilling fluid and low borehole temperature resulted in optimum log quality.

COMPARING WIRELINE AND CORE DERIVED ELEMENTS

The ECS irradiates the borehole and near wellbore formation with high energy neutrons from an Americium-Beryllium source and records the induced spectra, typically every six inches. The spectra include contributions from inelastic and capture interactions from about twenty elements present in the solid part of the formation, the pore space and the borehole. The derived capture elements are generally considered to be more accurate than the inelastic elements, but there are examples in the literature of inelastic carbon from the ECS being useful for interpretation. In general, elements present in the borehole and pore space, such as hydrogen, chlorine and oxygen, are ignored as it is difficult to separate out the borehole effect. Processing includes

compensation for the signal from iron in the tool and sulfur in barite mud. These algorithms are not discussed here.

For our purposes, the processing chain starts with the twenty relative capture yields stripped from the spectra. Two stripping algorithms were used by Schlumberger, the standard WALK2, and the more detailed ALKNA that may be used to strip for additional elements if data quality warrants its use.

The table to the right lists some of the differences between the two algorithms. The data presented here are from the ALKNA processing run by Schlumberger specialists familiar with the local geology.

It is important to appreciate that neither spectroscopy logging nor laboratory measurements directly yield absolute elemental fractions. Both methods yield relative fractions of the various elements, and these are transformed from relative yields to absolute weight fractions by means of a closure model. Closure models are simple conceptually but their appropriate application is very challenging in complex mineralogy, and they make certain assumptions about the earth's chemistry. The purpose of the closure model is to transform relative fractions to absolute mass fractions by accounting for the elements present in the earth (principally oxygen) that although measured, cannot robustly be partitioned between borehole, pore fluids and the solid part of the formation.

WALK2	ALKNA
Aluminum is estimated from iron, silica and calcite yields with optional adjustment for sulfur in pyrite.	Aluminum is stripped from capture spectrum.
Iron yield includes contribution from aluminum. $Fe_{WALK2} = Fe + 0.14 \times Al$	Iron and aluminum yields represent pure elements.
Calcium yield includes contributions from magnesium and sodium. $Ca_{WALK2} = Ca + 1.6 \times Mg + 0.6 \times Na$	Separate yields for calcium, magnesium and sodium
Potassium yield is in spectral analysis, but not used in closure or output.	Potassium yield is quantified.

A simple closure model for clastic environments assumes that the principal earth forming elements are present as oxides, for example SiO_2 , Al_2O_3 , Fe_2O_3 , Na_2O , K_2O , CaO , MgO , TiO_2 , MnO , etc. This is clearly appropriate for quartz. Applying these oxide ratios to orthoclase, KAlSi_3O_8 , one of the more common minerals present in clastic reservoirs, leads to the association of eight oxygen atoms with the potassium, aluminum and silicon (0.5 with K, 1.5 with Al and 2 with each of the 3 Si atoms) precisely as in the formula. These oxide associations are precise or close for common feldspars and clays, recognizing that there is some variability in their composition. The term “association factor” is used to denote the ratio of the oxide molecular weight to the weight of the root element. For example, for SiO_2 , the association factor is given by the ratio of the molecular weight of SiO_2 to the atomic weight of Si,

$$\frac{(28.0855 + 2 \times 15.9994)}{28.0855} = 2.139 \quad (1)$$

In carbonates, more appropriate associations would be CaCO_3 and MgCO_3 . If sulfur were only present in anhydrite (CaSO_4) the sulfur association would be set to account for the difference between the weights of CO_3 , ($12 + 3 \times 16 = 60$) already associated with Ca, and SO_4 ($32.06 + 4 \times 16 = 96.06$). The difference between 96.06 and 60 is 36.06 which is 1.126 times the atomic weight of sulfur, leading to a sulfur association factor of 1.126 for the case that sulfur is only present in anhydrite. However, if sulfur is also present in pyrite, the association factor would be selected such that it corrects for the Fe_2O_3 assumption for the iron in pyrite.

Some scenarios have no obvious rigorous answer. For example, the Green River Formation has an average of about 10 percent plagioclase for which the Na_2O association factor of 1.35 is appropriate, but also has intervals rich in Nahcolite (NaHCO_3) for which the association factor is 3.654.

Closure models used for wireline spectroscopy are discussed in more detail by Grau et al., 1989 and Herron et al., 1993. Note their use of adaptive logic for some elements.

Organic matter does not lend itself to characterization as oxides, or carbonates. Although the organic matter may be quantified and accounted for in the laboratory as part of the chemical analysis, this is not generally done with spectroscopy logs, so that while the results from the lab represent the mass fraction of the whole solid part of the formation, the spectroscopy logs quantify the mass fractions in the inorganic solid part of the formation. In most environments where organic matter is a small part of the formation, this distinction is unimportant. It cannot be ignored in very rich source rocks such as the Green River Shale.

The preceding discussion is intended to illustrate several points.

- Transforming relative elemental yields to absolute mass fractions requires some knowledge of the mineralogy. In mixed clastic-carbonate or other complex environments there is no perfect answer, though study of the core-derived mineralogy should help optimize the closure model. This applies to core- and wireline-derived elements.
- Discrepancies between core and wireline mass fractions result from applying different closure models to perfectly accurate relative yields. Comparison of the two is meaningless unless the closure models used in the two cases are understood and reconciled. Wireline log processing may include adaptive logic in the detailed application of the closure model.
- If wireline and core derived results agree, they may both be wrong if the same inappropriate closure model was used. The frequently misused assertion that core data represent “ground truth” does not apply here.

It follows that comparison between wireline and core derived elements should start by comparing ratios between elements as these do not rely on the assumptions inherent in a closure model or the different treatments of organic matter in the core and wireline transformations from relative to absolute quantities.

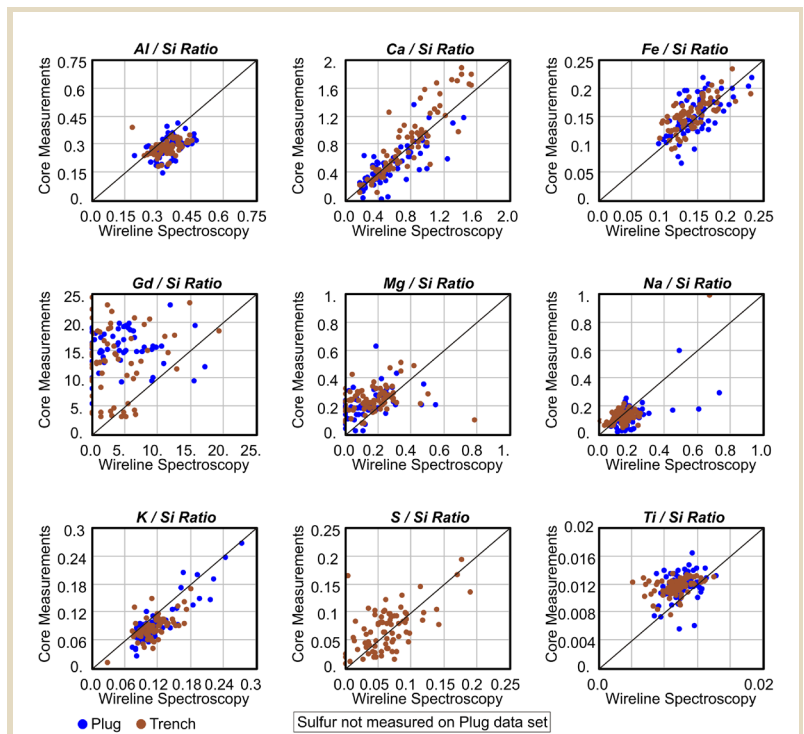


Fig. 1 Ratios of Core and wireline derived elements. Note the bias in the aluminum, magnesium, potassium and titanium ratios, and the poor agreement observed for gadolinium. There appears to be slightly less scatter in the trenched sample data, presumably due to the sampling difference. The 45° lines are drafted, not curve fits.

Ratios of all elements to silicon were computed for the spectroscopy and two core (plugs and trenched samples) data sets. Figures 1 and 2 show the comparison versus depth and as cross-plots. Knowing the oxides used for the XRF closure model (SiO_2 , Na_2O etc.) the core derived oxide fractions can easily be transformed to their corresponding elements. In addition to any shortcomings of the wireline and core measurements, scatter is caused by the difference in volume sampled by the plugs, the approximately six inch trenched samples, and the wireline measurements. These comparisons give us no reason to favor either core or wireline measurements. As expected, the wireline logs matched the trenched samples better than the plug off-cuts.

Dealing with organic matter

The comparisons between wireline and core derived elemental ratios show variable correlation, some biases, but no major discrepancies, with the exception of the gadolinium comparison that was not used for further analysis because gadolinium is not associated with any of the minerals solved for. No calibration shifts were made to any of the spectroscopy derived elements at this stage.

There are two reasons why agreement between core and wireline derived elemental ratios to silicon does not necessarily lead to a perfect match of elemental concentrations. Both are due to processing differences applied to the two data.

1. The wireline-derived elements are fractions of the inorganic part of the solid rock, while the core measurements are fractions of the dry rock including organic matter.
2. Different closure models are used. A simple oxide closure model was used for the core data set, while the wireline processing used associations intended to represent the known chemistry of the Green River Formation.

In order to use the wireline derived elemental yields quantitatively in a conventional compositional analysis of the relative volumes of minerals and fluids in the whole formation, they need to be transformed from dry weight fractions of the solid inorganic part of the formation to weights per unit volume of the whole formation. This requires an estimate of the volume or weight fraction of organic matter, the standard for which is the measurements made on core as part of the QXRD suite.

USING ELEMENTS IN PETROPHYSICAL ANALYSIS

The basic premise of detailed compositional analysis is that quantification of the minerals in the formation improves prediction accuracy of the hydrocarbon resource, whether free liquid or gas-

eous hydrocarbon or, in our case, oil shale liquid potential. The reasoning is simple—porosity estimation in traditional log analysis relies heavily on the density log, and computed porosity is dependent on the accuracy of the grain and fluid densities used in the computation. In this case the situation is awkward. Inorganic mineralogy is complex and quantifying it requires reference to the spectroscopy data. The dry weight yields delivered from spectral stripping followed by the application of a closure model represent fractions of the solid part of the formation less organic matter. Although the spectra include contributions from the organic matter in the carbon, oxygen and hydrogen yields, these do not lend themselves to use in a hypothetical closure model that includes organics.

- Carbon's presence in carbonates would have to be accounted for by reference to the calcium, magnesium and sodium yields. This is not infeasible, but in any

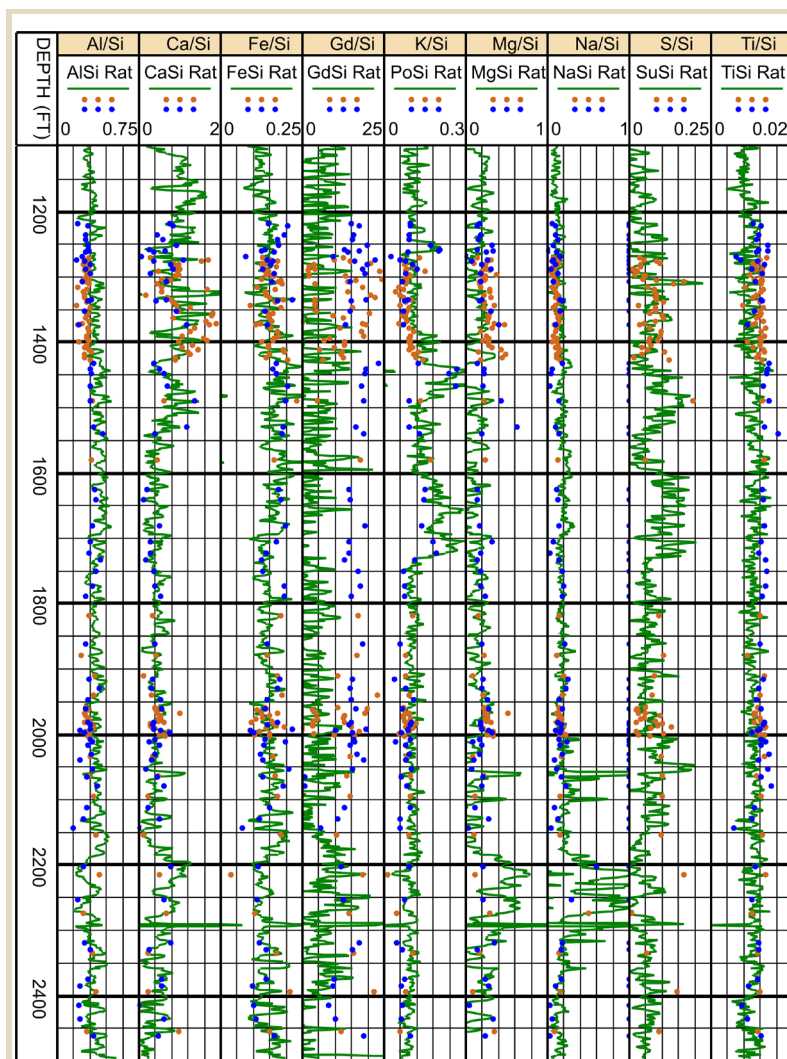


Fig. 2 Wireline and core derived elemental ratios. Plug off-cut samples are plotted blue and trenched samples brown. Sulfur was not measured on the plug off-cuts.

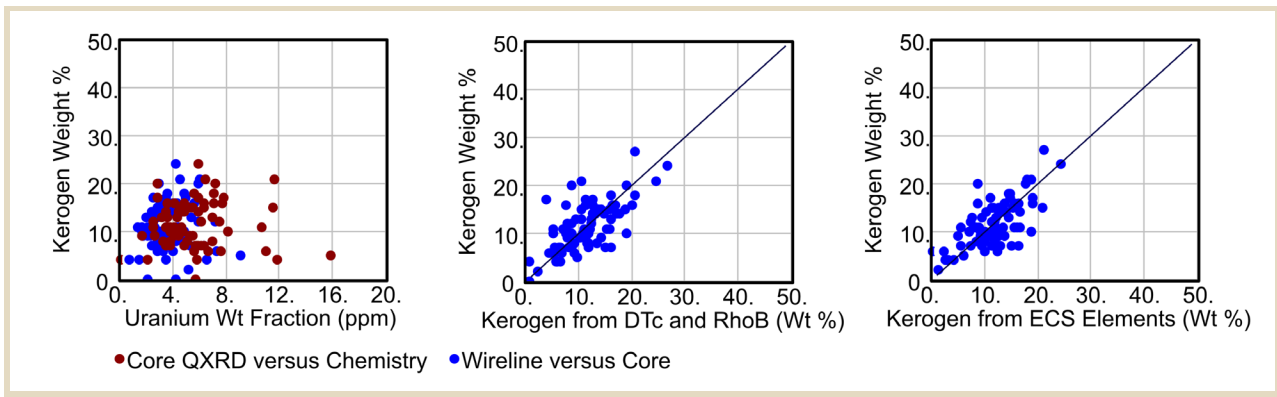


Fig. 3 Kerogen prediction from spectroscopy logs and square root conductivity, density and sonic logs. No correlation was attempted with uranium from natural gamma spectroscopy.

case the carbon yield is inelastic, and therefore represents a different volume from the capture elements.

- Oxygen is an inelastic yield, and includes contributions from the borehole, porosity, formation water and inorganic minerals.

- Hydrogen is also present in the borehole, formation water, Nahcolite and clays.

Incorporating organic matter into a future closure model has not been ruled out, but is not pursued here. In order to transform the dry weight capture elements to fractions of the whole solid part of the rock, it was necessary to first quantify the organic matter. Several methods were considered and results are cross-plotted on Figure 3 and shown versus depth in Figure 4.

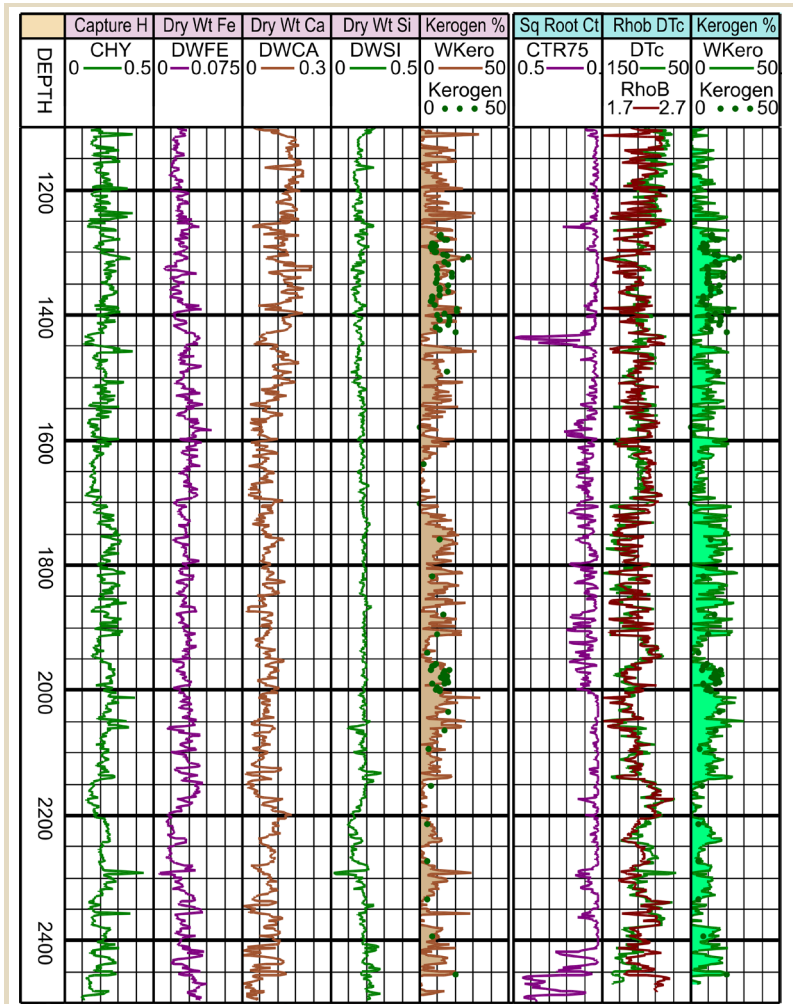


Fig. 4 Kerogen prediction from spectroscopy log-derived H, Fe, Ca and Si (mnemonic WKero_ECS) and square root conductivity, density and sonic log (mnemonic WKero_RMA). Visually, the predictions are similar.

Prediction from the natural gamma uranium yield, taking advantage of a frequently observed correlation

Little or no correlation was observed when plotting kerogen from XRD against both wireline and core derived uranium.

Prediction from commonly run logs—in this case deep resistivity, sonic and density

Using either of density and compressional sonic in combination with resistivity is analogous to Passey’s (1990) method, adapted for the case where there is no baseline corresponding to the absence of organic matter. The deep resistivity log was first transformed to square root conductivity at a standard temperature of 75° F in order to make it more linear with respect to the other logs and remove the effects of temperature variations. Details are explained in the section “DIRECT ESTIMATION OF LIQUID YIELD.”

A slightly better correlation ($r^2 = 0.473$) was obtained using all three of square root conductivity, compressional slowness and bulk density than any subset. The resulting formula derived by multiple linear regression was

$$W_{Kerogen} = \tag{2}$$

$$15.027 - 31.03 \times CTr75 + 0.277 \times DTc - 16.20 \times \rho_b .$$

Predicting by multiple linear regression from a combination of the capture spectroscopy yields

Various combinations were considered and the hydrogen yield was found to correlate most closely. Other elements and NMR porosity, chosen to mitigate the effects of hydrogen in the borehole and porosity, were tested. The best correlation ($r^2=0.5408$) was achieved with the following formula:

$$W_{Kerogen} = -37.43 + 137.7 \times CHy + 444.8 \times dwfe + 44.05 \times dwca \quad (3)$$

This is a purely statistical correlation. The raw capture hydrogen yield was found to correlate better than the product of capture hydrogen and the yields to weights conversion factor. Chlorine, considered as it could potentially compensate for water in the borehole or formation, and porosity did not improve the correlation. This ECS elements based correlation was the best obtained and achieved a higher correlation coefficient that was obtained with the other two approaches considered. See Figures 3 and 4.

Having estimated the kerogen weight fraction, the dry weight fractions from spectroscopy are transformed to weight fractions of the whole solid rock by dividing by $(1 + W_{Kerogen})$. For example, for iron, $WWFE = DWFE / (1 + W_{Kerogen})$ where $WWFE$ is the weight fraction iron in the whole solid rock. After this transformation, the ECS elements are more analogous to the core data, though they still differ in the closure models used for the two datasets. Element fractions before and after transformation are compared with core

Mineral	Max	Min	Mean
1 Ankerite	62	1	28.0
2 Quartz	51	2	15.5
3 Kerogen	27	0	11.3
4 Plagioclase	23	0	8.6
5 K-Feldspar	21	0	7.0
6 Dawsonite	29	0	6.6
7 Total Clay	39	0	5.8
8 Buddingtonite	18	0	5.4
9 Calcite	29	0	4.2
10 Aragonite	31	0	3.5
11 Nahcolite	75	0	1.8
12 Pyrite	5	0	1.0
13 Siderite	5	0	0.5

data on Figure 5. Note that the biases observed with the ratio data are still present. Fractions of the inorganic part of the rock (mnemonics DWxx) are plotted green, and fractions of the whole dry rock are plotted black (mnemonics WWxx).

DETAILED MINERALOGICAL ANALYSIS

A simple comparison between wireline spectroscopy and core derived mineralogy may be made in the massive domain, considering only the solid fraction of the rock. The table below lists the principal minerals present in decreasing order of abundance, as determined from XRD. Ignoring gadolinium and titanium that are not present in any of these minerals we have a total of eight elements from spectroscopy, plus the kerogen weight fraction calculated previously, plus the implied unity equation for a total of ten equations.

The chemical formulae and therefore the weight fractions of many common minerals are somewhat variable in

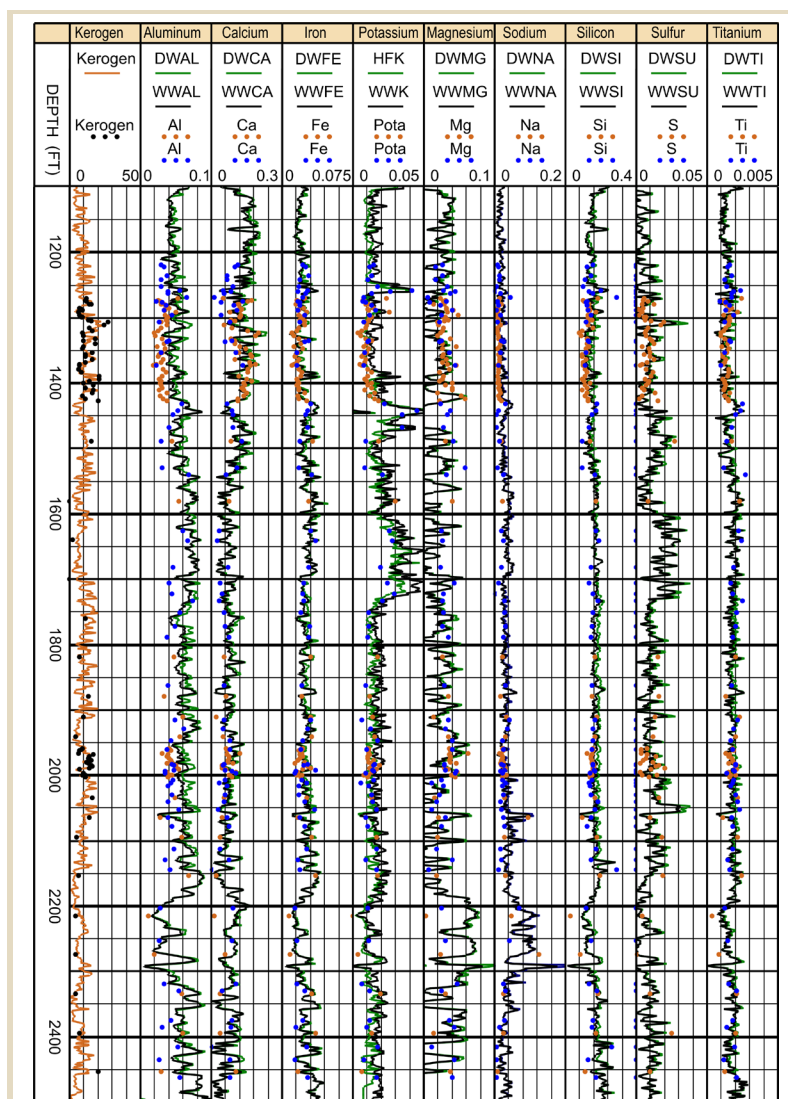


Fig. 5 Transforming elements to fractions of solid rock including kerogen. Plug off-cut samples plotted blue and trench samples brown.

TABLE 2: Chemical formulate determined by BestRock (lower interval).

Mineral	Formula
Quartz	SiO ₂
Aragonite	CaCO ₃
Nahcolite	NaHCO ₃
Dawsonite	NaAl(CO ₃)(OH) ₂
Pyrite	FeS ₂
Organic Matter	Unknown
Siderite	Ca _{0.02} Mg _{0.21} Fe(II) _{0.75} Mn _{0.02} CO ₃
excess-Ca Dolomite	Ca _{1.05} Mg _{0.90} Fe(II) _{0.05} Mn _{0.00} (CO ₃) ₂
Calcite	Ca _{1.00} Mg _{0.00} CO ₃
K-feldspar	K _{0.97} Na _{0.03} AlSi ₃ O ₈
Na-plagioclase	K _{0.05} Na _{0.85} Ca _{0.10} Al _{1.10} Si _{2.90} O ₈
Buddingtonite	K _{0.20} (NH ₄) _{0.80} AlSi ₃ O ₈
Illite-Smectite	(K _{0.71} (NH ₄) _{0.05} Na _{0.00} Ca _{0.04})(Al _{1.47} Fe(II) _{0.00} Fe(III) _{0.34} Mg _{0.18})(Si _{3.34} Al _{0.66})O ₁₀ (OH) ₂

nature. By combining elemental and mineralogical data, locally optimized chemical formulae, and hence elemental weight fractions and other log responses may be determined. This was achieved using Chevron’s proprietary BestRock (Derkowski et al., 2008) program. BestRock takes mineral concentrations from X-ray diffraction, bulk rock elemental data from X-ray fluorescence (XRF) or inductively coupled plasma (ICP) and cation exchange capacity as inputs, and uses a non-linear optimizer to solve for the elemental concentration of each mineral. Some minerals such as quartz are assumed to have the well known formulae of the pure mineral, while elemental concentrations in minerals such as feldspars and calcium-magnesium carbonates are considered unknown and optimized.

In this case, there are two intervals with somewhat different mineralogical assemblages, so the program was run twice, to solve separately for the properties above and below 1800 ft measured depth. The upper interval is characterized by abundant plagioclase, CaCO₃-related minerals, low dawsonite and low quartz. The lower interval has low plagioclase, little aragonite and calcite, abundant dawsonite and locally high concentrations of nahcolite. See Table 2 for the optimized formulae determined by this process, and Table 3 for the corresponding weight fractions for each element in the minerals. Note that these are partial lists—rare minerals such as anatase, apatite, fluorite etc. are omitted from the table.

It is unrealistic to distinguish minerals such as calcite and aragonite from wireline logs, so these were lumped together, leaving a total of 12 minerals to solve for with eight elemental yields (Si, Al, Ca, Mg, K, Fe, S and Na), plus the separately determined organic matter estimate, and the implied unity equation. This is an under-determined situation that

may be addressed by either solving for fewer minerals, by ignoring the less abundant, or by using additional log data.

Additional elements—for example thorium and uranium from natural spectral gamma, and titanium and gadolinium from the ECS were found not to correlate with the more abundant minerals, and so were not considered.

VOLUMETRIC DOMAIN INTERPRETATION

Working in the more familiar volumetric domain enables us to additionally use the conventional logs such as density, volumetric photoelectric cross section and NMR porosity.

Addition of the eight elements from spectroscopy, kero-gen fraction, density, photoelectric cross section and total porosity from NMR and implied unity brings the total number of input curves to 13. This compares with 12 solids plus porosity. Petrophysical analysis is therefore mathematically possible.

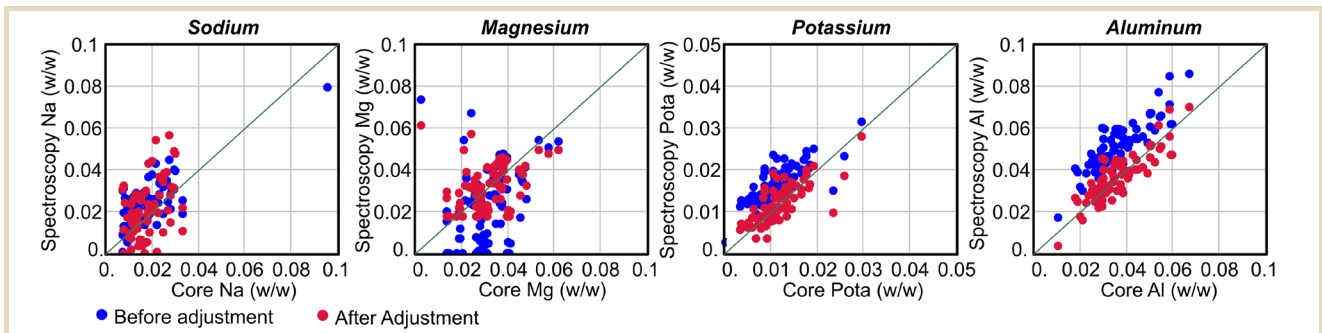
In order to use the elemental and kerogen weight fractions in a quantitative analysis in the volumetric domain, they need to be transformed from grams of element *x* per gram of solid rock to grams of element *x* per cubic centimeter of whole formation. The transformation is illustrated using iron as an example. The weight of iron in one cubic centimeter of whole formation is given by $WVFE = WWFE \times (1 - \phi) \times \rho_{grain}$. Consider this as grams of iron per cubic centimeter of formation.

A continuous total porosity curve from the NMR partitions solids from fluids volumetrically, and enables grain density to be computed from bulk density and porosity using $\rho_{grain} = \rho_{bulk} - \phi \times \rho_{fluid} / (1 - \phi)$.

This transformation between domains is handled internally by several commercial log analysis applications, but may equally be done explicitly by the user.

TABLE 3: Log interpretation data.

Mineral	Si	Al	Ca	Mg	Na	K	Fe	S	U(b/cm ³)	ρ_b (g/cm ³)
Quartz	46.7								4.92	2.65
Nahcolite		18.7			16.0				1.68	2.223
Dawsonite					27.4				2.53	2.437
Pyrite							46.6	53.4	87.11	5.013
Siderite			0.8	4.7			32.5		40.67	3.88
Organic Matter								2.7	0.37	1.0
excess-Ca Dolomite									13.9	2.926
Calcite			40.0	0.0					15.1	2.81
K-feldspar	30.3	9.7			0.2	13.7			8.94	2.518
Na-plagioclase	30.8	11.2	1.5		7.4	0.7			6.03	2.631
Buddingtonite	31.2	10.0				2.9			3.62	1.701
Illite-Smectite	23.5	14.4	0.4	1.1	0.0	7.0	4.8		10.84	2.86

**Fig. 6** Adjustment of wireline spectroscopy elements to improve match to core.

Recall that BestRock gives apparent log response parameters that are consistent with the core data alone. Any calibration biases between log and core data would result in inconsistent results when using these results for compositional analysis. Consequently the elements showing significant biases on Figure 5, aluminum, potassium, magnesium and sodium, were first adjusted using coefficients determined by least squares regression. Crossplots of these four elements before and after adjustment are shown on Figure 6. We stress that this adjustment is not based on a belief that the core data are a standard which wireline data should be forced to match. It is a necessity if computations using wireline measurements are to deliver mineralogy consistent with core data using the response parameters from BestRock.

Initial tests of the model made up of 13 equations and 13 unknowns resulted in variable matches to core. In particular, the logs had difficulty distinguishing plagioclase, buddingtonite and dawsonite. This is not surprising given their similar aluminum and sodium concentrations.

Reference to the core-derived mineralogy indicates that mineral distribution varies between the upper and lower sections. Plagioclase is abundant in the shallower section, but

almost absent in the lower part, where dawsonite is more prevalent. Two alternative models were run, with nahcolite absent from the model used in the upper interval. Nahcolite in the model reduced the computed plagioclase volume. The two models were merged over the interval from 1600 to 2000 ft measured depth over which the plagioclase fraction reduces. See Figure 7 for a plot showing the additional logs, the mineralogy from QXRD plotted as weight fractions of the solid rock and volume fractions of the whole formation, and the results of running various log analysis models. The headed “Combined” track shows a final result achieved by combining the individual models. Details of the log interpretation models are shown in table 2.

TRANSFORMING KEROGEN FRACTION TO LIQUID HYDROCARBON YIELD

Compositional analysis yields an estimate of kerogen fraction. Conventional wisdom states that liquid yield is proportional to kerogen fraction. The correlation between Fischer Assay (FA) results and kerogen from X-ray diffraction made on off-cuts from the same samples is shown on

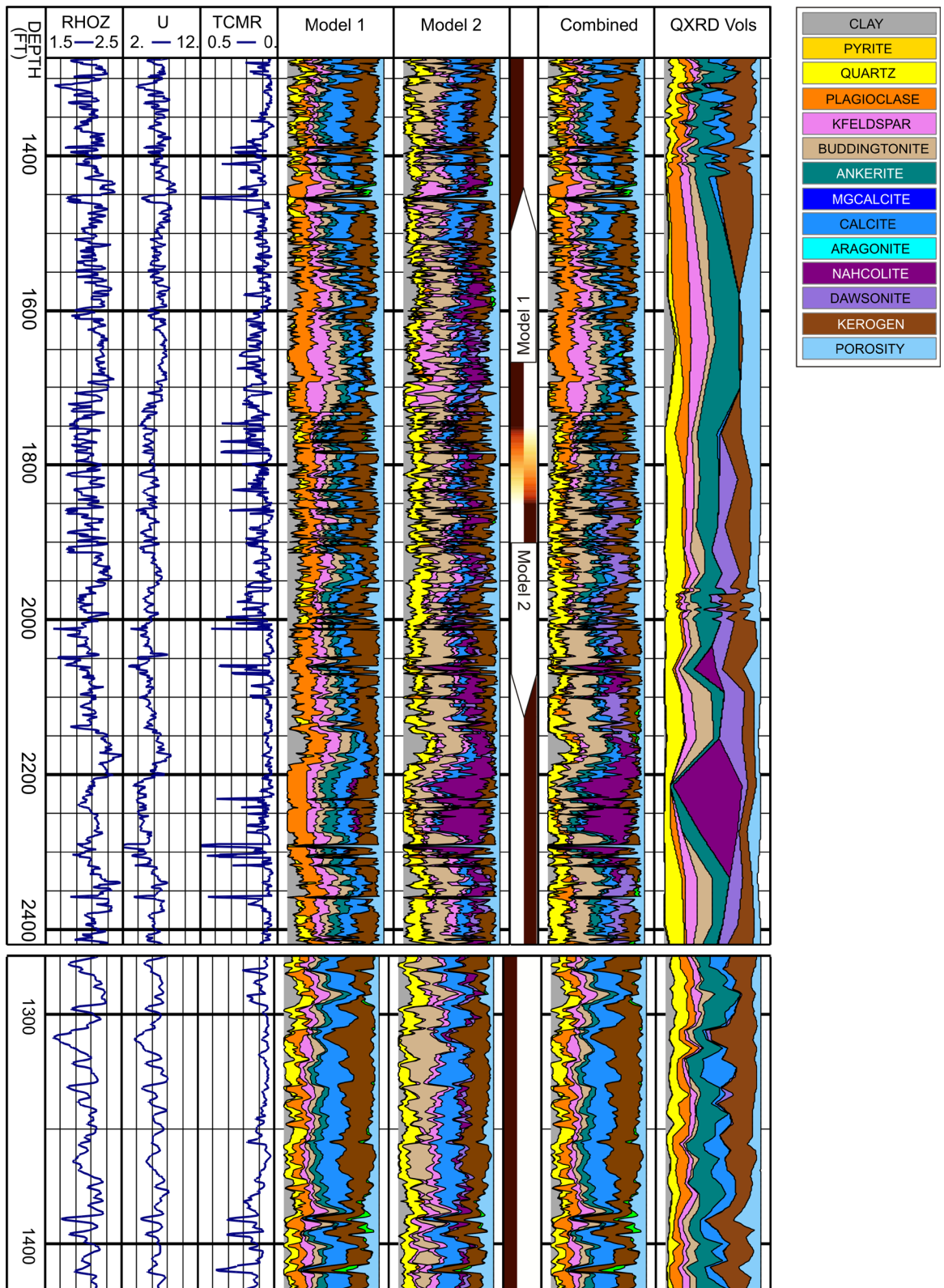


Fig. 7 Input curves, individual models, combined model and QXRD presented as volume fractions. The lower figure shows the interval with dense QXRD and ICP sampling.

Figure 8. The correlation is rather poor, prompting questions about the integrity of the FA measurements. Consequently, the correlation between FA and RockEval estimates was examined. This uses a much smaller sample and somewhat different procedure and temperatures. The indication is that kerogen fraction is not very well correlated with liquid hydrocarbon yield. There are many possible reasons for this, including limitations in our ability to quantify kerogen from core analysis, and the possibility that its properties vary somewhat. If the latter is true, it calls the detailed volumetric analysis into question as this approach assumes constant properties for the components.

Nonetheless it implies that there is potential value in a direct estimate of hydrocarbon yield or, to put it another way, a method to reproduce Fischer Assay results.

DIRECT ESTIMATION OF LIQUID YIELD

Passey and Creaney (1989) proposed an overlay construction to estimate total organic carbon (TOC) in kerogen for application to shale gas reservoirs. Similar reasoning may be applied to estimate oil yield from kerogen-rich rocks. It is presented in a modified form intended to make the method easier to apply in general, and possible in our case where organic matter is present throughout the interval, preventing the identification of the required kerogen-free baseline.

The idea behind Passey's correlation is that in water bearing rocks with essentially constant mineralogy, the resistivity and porosity logs (density, sonic and neutron)

correlate. Higher water-filled porosity corresponds to lower resistivity. Replacing some of the shale with non-conductive organic matter increases resistivity slightly because less clay bound water is present. It increases the apparent porosity because organic matter has a lower density and velocity than shale. The width of the resulting gap between the two curves indicates the quantity of organic matter.

Recourse to the Archie equation for wet rocks, with a cementation exponent m of 2, illustrates that porosity is proportional to the square root of conductivity C_t , where R_w and C_w are the resistivity and conductivity of the formation water, and ϕ is porosity.

$$1 = \frac{1}{\phi^2} \frac{R_w}{R_t} \quad \phi^2 = \frac{C_t}{C_w} \quad \phi \propto \sqrt{C_t} \quad (4)$$

Changes in water resistivity due to salinity and temperature variations affect the correlation quality. The temperature effects may be compensated for by applying the Arps formula to transform the observed resistivity R_t recorded at a borehole temperature of $T^\circ\text{F}$ to a standard temperature, say 75°F .

$$\frac{1}{C_{t_{75}}} = \frac{T + 6.77}{C_t(75 + 6.77)} \quad (5)$$

Since the response of the common porosity logs is loosely proportional to porosity, a linear correlation may be expected between square root conductivity C_{tr} and the density and sonic logs. Whereas Passey overlaid a logarithmically scaled resistivity on the porosity logs, we overlay square root conductivity, transforming the estimation of the gap between the curves due to organic matter to a simple linear problem.

In most unconventional plays it is possible to identify a correlation corresponding to zero organic matter. This is not possible in the Green River formation because organic matter is present throughout the interval of interest. However, if the porosity log is proportional to C_{tr} in the absence of organic matter, and the effect of organic matter on the two logs is linear, the problem may be recast as a multiple linear regression of C_{tr} and either density ρ_b or compressional slowness DTc .

$$\text{FA Oil Yield} = a + b \times C_{tr75} + c \times \text{RhoB} \quad (6a)$$

$$\text{FA Oil Yield} = d + e \times C_{tr75} + f \times DTc \quad (6b)$$

Cross-plots of density and DTc against C_{tr} at 75°F , colored by the Fischer Assay, results in weight percent are shown on Figure 9. Increasing oil yield moves data points to the northwest and similar oil yields form bands lying in the southwest-northeast direction. Lines corresponding to zero oil yield derived from the regression coefficients are shown.

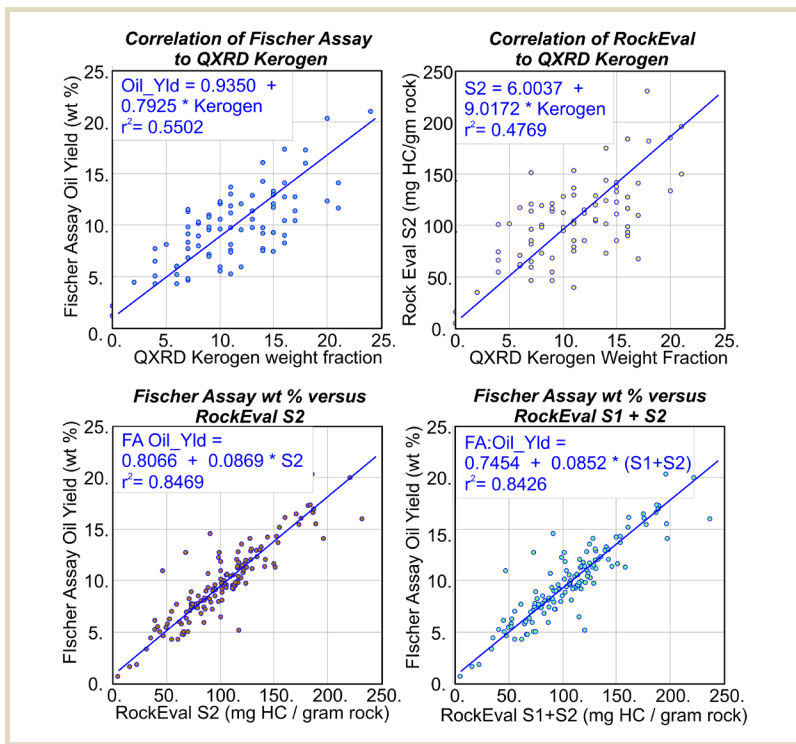


Fig. 8 Fischer Assay liquid hydrocarbon yield versus kerogen from core data and RockEval pyrolysis.

Using Passey’s method, these would normally be derived by inspection of the data from kerogen free intervals.

The results of the two regressions for oil yield in weight percent were correlation coefficients r^2 close to 0.5 and the following coefficients:

$$\text{Oil_Yield_from_RhoB}(wt\%) = 70.7544 - 25.1979 \times \text{Ctr75} - 28.7501 \times \text{RhoB} \tag{7a}$$

$$\text{Oil_Yield_from_DTc}(wt\%) = -21.4153 - 61.7341 \times \text{Ctr75} + 0.3067 \times \text{DTc} \tag{7b}$$

Applying these two formulae, we generated continuous estimates of oil yield that were transformed to gallons per ton using the conversions in ASTM D3904 and the mean oil density from Fischer Assay of 0.891 g/cm³.

$$\text{Oil_Yield_from_DTc}(GPT) = \text{Oil_Yield_from_DTc}(wt\%) \times 2.397 / 0.891 \tag{8a}$$

$$\text{Oil_Yield_from_RhoB}(GPT) = \text{Oil_Yield_from_RhoB}(wt\%) \times 2.397 / 0.891 \tag{8b}$$

To convert these to the more familiar oilfield units “barrels per acre-foot” the grain density and porosity of the rock need to be known. These were derived from the NMR and density logs. To transform the FA sample weight to a dry weight, subtract the weight of water given off during the test and recompute the oil yield as a fraction of the dry rock, noting that the liquid hydrocarbon is (perversely) considered part of the dry rock. The liquid driven off is treated as an indeterminate part of the total porosity as the sample is assumed to be partially drained.

$$\text{Dry_oil_yield_1}(ml/grams\ dry\ rock) = \text{Oil_Yield_}\% / ((100 - \text{Water_Yield_}\%) \times \text{Rho_Oil}) \tag{9}$$

Volumetric oil yield in v/v units in the dry rock is given by

$$\text{Dry_oil_yield_2}(v/v\ units\ of\ dry\ rock) = \text{Dry_oil_yield_1} \times \text{Grain\ Density} \tag{10}$$

Volumetric oil yield is whole rock in v/v is

$$\text{Oil_Yield_Whole_Rock}(v/v\ of\ whole\ formation) = \text{Dry_oil_yield_2} / (1 - \phi_T) \tag{11}$$

The above is equivalent to hydrocarbon filled porosity $\phi_T \times (1 - S_w)$ in conventional reservoirs. To convert to barrels per acre-foot, multiply the whole rock volume by the

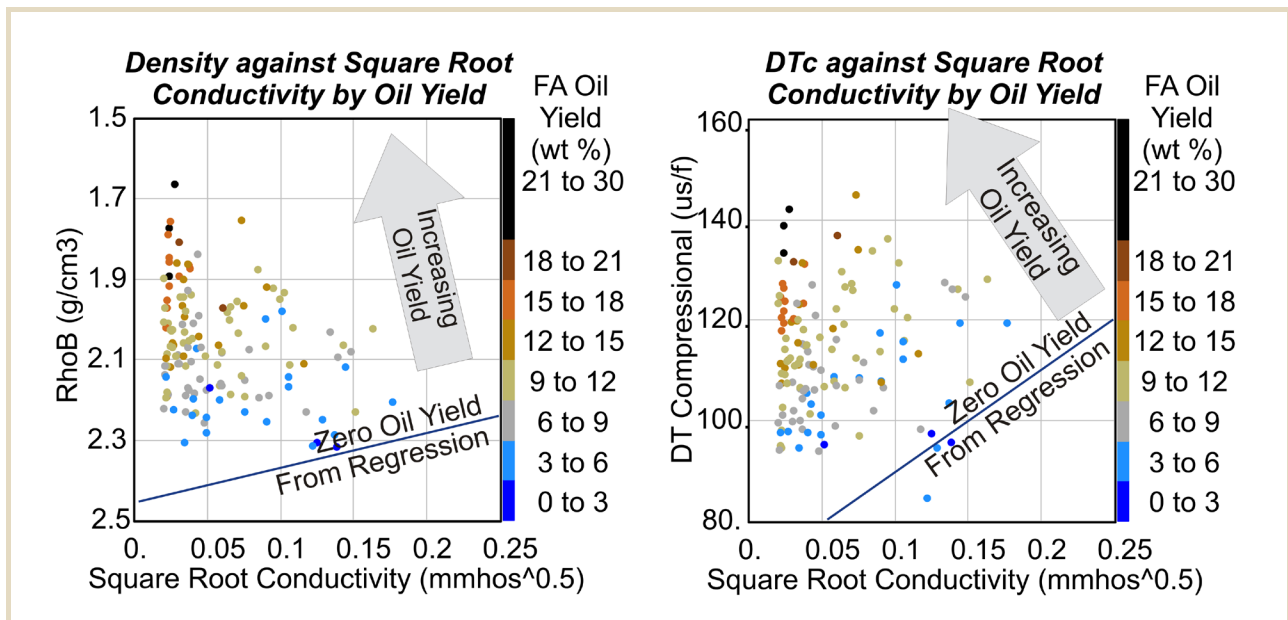


Fig. 9 Direct estimation of liquid hydrocarbon yield from square root conductivity and either density or compressional sonic logs. Data points are colored by Fischer Assay oil yield and form loose bands parallel to the diagonal lines corresponding to zero organic matter.

number of cubic feet per acre-foot and divide the hydrocarbon fraction by the number of cubic feet per barrel of liquid.

$$1 \text{ acre} = 43560 \text{ square feet and } 1 \text{ barrel} = \tag{12}$$

$$42 \times 0.133680556 = 5.614583 \text{ cubic feet}$$

$$\text{Oil_In_Place (bbl/acre-foot)} = \tag{13}$$

$$\text{Oil_Yield_Whole_Rock} \times 43560 / 5.614583$$

In the absence of any known evidence to the contrary, this analysis assumes that the liquid hydrocarbon distilled from the assay had the same volume when associated with the kerogen—the organic matter behaves like a wet sponge.

Because this is essentially a statistical correlation, it could equally have been done by converting the Fischer Assay results to barrels per acre-foot using the same method, and referring to the density and porosity logs as before, and running a similar regression against the resistivity, sonic and density logs.

The results are plotted on Figures 10 and 11. Note that both correlation coefficients are close to 0.5. Averaging the two predictions (not shown) improved the correlation coefficient to 0.54. Recall the correlation coefficient of 0.473 found earlier when estimating kerogen from the same logs as part of the input to the petrophysical analysis. Assuming that our aim is to reproduce core data, we can do a better job of reproducing liquid yield than kerogen fraction, and this direct approach does not rely on a further correlation between kerogen and liquid yield.

CONCLUSIONS

Comparisons were shown between wireline spectroscopy and core derived elemental measurements. These were initially presented as ratios to avoid incompatibilities due to the different closure models used in the two cases. The comparisons vary in quality, and some biases were evident.

These comparisons are not representative of all data sets. In cases with simpler mineralogy, such as carbonate-evaporite sequences, the wireline elemental measurements should be expected to be more accurate. Nonetheless, locally derived core-based chemistry is valuable.

Because the standard wireline spectroscopy measurements represent fractions of the inorganic part of the solid rock, it was necessary to independently estimate the organic fraction of the rock in order to use these data in conventional volumetric log interpretation.

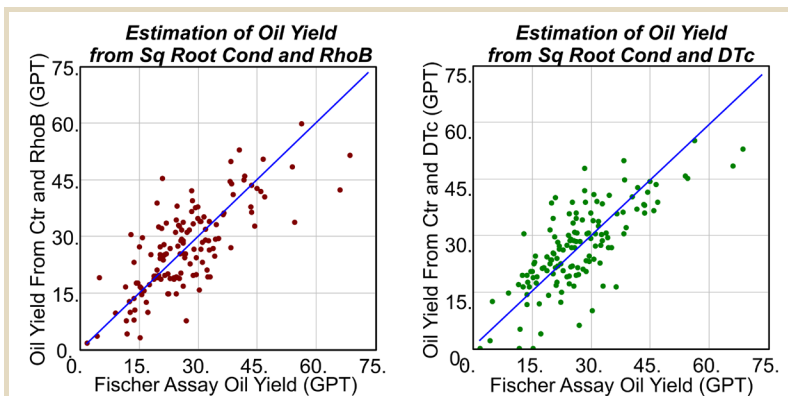


Fig. 10 Comparison of observed (Fischer Assay) and predicted oil yields in gallons per ton.

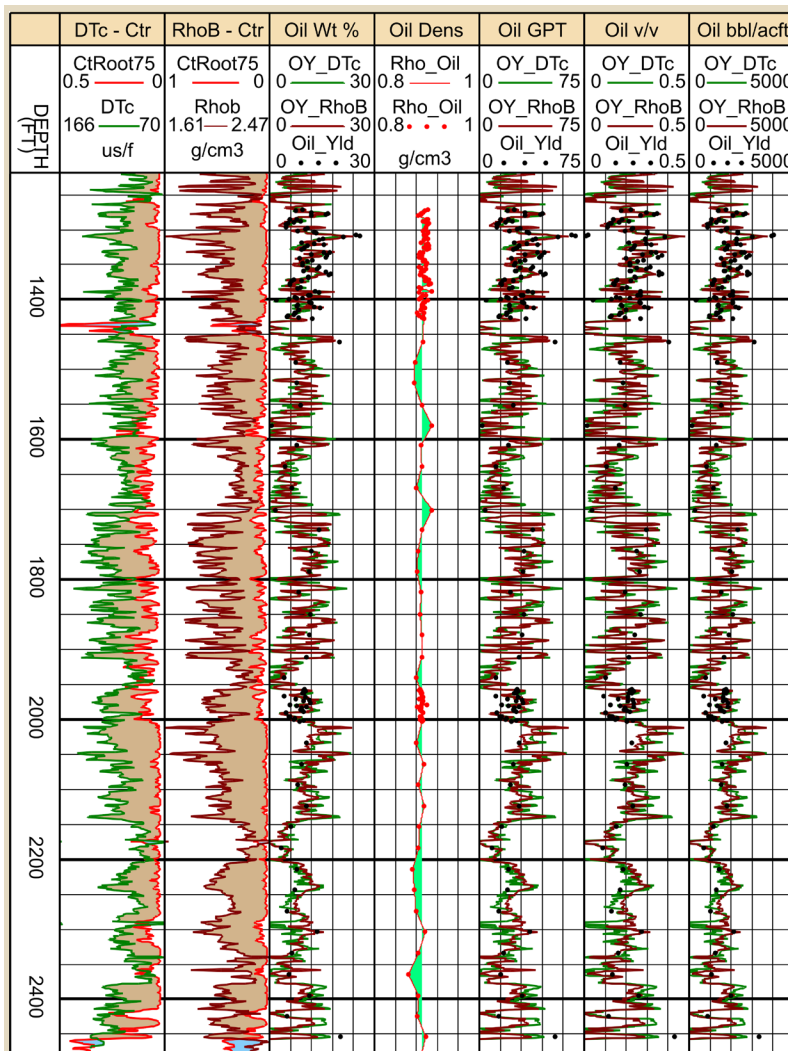


Fig. 11 Reproduction of Fischer Assay liquid yields using conventional logs.

Reproducing the complex mineralogy observed on core data with the spectroscopy logs was a challenge. Distinguishing the three feldspars (plagioclase, K-feldspar and Buddingtonite) and various carbonates (aragonite, excess Ca-dolomite, ankerite and siderite) was particularly difficult. Two separate models were needed to handle the separate assemblages of minerals in the upper and lower sections.

There is clearly potential for further developing and streamlining workflows for using spectroscopy data in formations where the organic matter represents or indicates the commercial resource.

RockEval gives very similar results to Fischer Assay, subject to local calibration. This is a useful observation as RockEval requires a much smaller sample. If the purpose of the exercise is to quantify liquid hydrocarbon potential and Fischer Assay represents the benchmark, better results are obtained by direct prediction than via an estimate of kerogen fraction and a detailed petrophysical analysis.

The data suggest that either kerogen properties are somewhat variable, or our estimates of kerogen fraction from core data are less accurate than our estimates of minerals with better defined XRD standards. In this case, detailed mineralogical evaluation benefitted from induced spectroscopy data.

ACKNOWLEDGEMENTS

The BestRock interpretation was run by Doug McCarty and Arek Derkowski of Chevron. Special thanks are due to Jim Grau of the Schlumberger Doll Research Laboratory for the ECS processing and for his patient and detailed explanation of the various closure algorithms used on this dataset and others that I have worked on over the past few years.

REFERENCES

ASTM D3904-90, 1990, Standard test method for oil from oil shale (resource evaluation by the Fischer Assay Procedure): American Society for Testing and Materials.

Derkowski A., McCarty D. K., Środoń J., and Eberl D. D., 2008, BestRock - mineralogy, chemistry, and mineral surface property optimization to calculate petrophysical properties of the mineral matrix: *Mineralogia - Special Papers*, vol. 33, p. 53.

Grau, J. A., Schweitzer, J. S., Ellis, D. V., and Herzog, R. C., 1989, A geological model for gamma-ray spectroscopy logging measurements: *Nuclear Geophysics*, vol. 3, no. 4, p. 351–359.

Herron S. L., Herron, M. M., Grau, J. A., and Ellis, D. V., 1993, Interpretation of chemical concentration logs and applications in the petroleum industry, Chapter 24, *Remote Geochemical Analysis: Elemental and Mineralogical Composition*, Ed. C.M. Peters and P.A. Englert, Cambridge University Press, p. 507–537.

Lewin M. and Hill R., 2006, Evaluating oil-shale product yields and compositions by hydrous pyrolysis: Colorado Energy Research Institute, presented at the 26th Oil Shale Symposium, Colorado School of Mines, Golden, Colorado, Oct. 16–20.

Manning, T. J. and Grow, W. R., 1997, Inductively coupled plasma–atomic emission spectroscopy: *The Chemical Educator*, vol. 2, no. 1.

Omotoso, O., McCarty, D. K., Hillier, S., Kleeberg, R., 2006, Some successful approaches to quantitative mineral analysis as revealed by the 3rd Reynolds Cup contest: *Clays and Clay Minerals*, vol. 54, no. 6, p. 748–760.

Passey, Q. R., Creaney, S., Kulla, J. B., Moretti, F. J., and Stroud, J. D., 1990, A practical model for organic richness from porosity and resistivity logs: *AAPG Bulletin*, vol. 74, no. 12, p. 1777–1794.

Środoń, J., Drits., V. A., McCarty, D. K., Hsieh, J. C. C., and Eberl, D. D., 2001, Quantitative x-ray diffraction analysis of clay-bearing rocks from random preparations: *Clays and Clay Minerals*, vol. 49, no. 6, p. 514–518.

Tissot, B. P. and Welte, D. H., 1984, *Petroleum Formation and Occurrence*, 2nd edition: Heidelberg Springer-Verlag Telos.

Van den Oord, R. J., 1991, Evaluation of geochemical logging: *The Log Analyst*, vol. 32, no. 1, p. 1–12.

ABOUT THE AUTHOR



Christopher Skelt has an MA in engineering from Emmanuel College Cambridge and an MSc in Bioengineering from the University of Strathclyde, Glasgow. He entered the oil industry in 1977 as a Schlumberger field engineer in South America. He has worked in petrophysics since 1984 with Schlumberger, Shell, Scott Pickford, LASMO, Unocal and Chevron.